

# DNS of Heat Transfer in a Transitional Channel Flow Accompanied by a Turbulent Puff-like Structure

T. Tsukahara<sup>1</sup>, K. Iwamoto<sup>1</sup>, H. Kawamura<sup>1</sup> and T. Takeda<sup>2</sup>

<sup>1</sup>*Department of Mechanical Engineering, Tokyo University of Science,  
Noda-shi, Chiba 278-8510, Japan, [a7599109, iwamoto, kawa]@rs.noda.tus.ac.jp*

<sup>2</sup>*Nuclear Science and Engineering Directorate, Japan Atomic Energy Agency,  
Oarai-machi, Higashi Ibaraki-gun, Ibaraki 311-1393, Japan, takeda.tetsuaki@jaea.go.jp*

**Abstract** — Direct numerical simulation of heat transfer in a fully developed channel flow has been carried out in a range of low Reynolds numbers from  $Re_\tau = 180$  to 60 with emphasis on the puff-like structure. For  $Re_\tau \leq 80$  with the largest box of  $51.2\delta \times 2\delta \times 22.5\delta$ , the turbulent puff in a channel is observed and significantly affects the momentum and heat transports. The spatial structure of the equilibrium puff is examined with taking account of two different thermal boundary conditions. It is revealed that there exists a localized strong turbulent region, in which the secondary flow is induced by the puff. In consequence, at the present lowest Reynolds number as low as  $Re_\tau = 60$ , the flow remains turbulent and the larger Nusselt numbers than those without puff is obtained.

## 1. Introduction

Heat transfer at a low Reynolds number in a turbulent/transitional channel flow is of practical importance with respect to a high temperature gas-cooled nuclear reactor, in which the low  $Re$  is employed to obtain a high outlet gas temperature with maintaining turbulence. Direct numerical simulation (DNS) is a significant tool for the investigation of the turbulent heat transfer in a channel. The first such DNS was made by Kim and Moin [1] with an assumption of uniform heat generation at  $Re_\tau = 180$ , where  $Re_\tau$  is based on a friction velocity  $u_\tau$  and a channel half width  $\delta$ . Later, the Reynolds- and Prandtl-numbers dependencies have been investigated by many research groups (e.g., Kawamura *et al.* [2]). On the other hand, not much work has been done on DNS of heat transfer in a turbulent/transitional channel flow for a lower Reynolds number than  $Re_\tau = 150$ . As for the transitional channel flow without a scalar transport, Iida and Nagano [3] carried out the DNS for  $Re_\tau = 60 - 100$  to investigate the mechanisms of laminarization. The authors' group [4] showed that by expanding the domain, a localized laminar-like structure was observed at  $Re_\tau = 80$ . The structure was found to be similar to the ‘puff’ in a transitional pipe flow studied by Wygnanski and Champagne [5].

In the present work, the heat-transfer statistics associated with fully developed scalar fields for two different thermal boundary conditions are presented and discussed with emphasis on the role of the puff-like structure in the scalar transport. A series of DNS has been made for  $Re_\tau = 60 - 180$  with the large computational box sizes as summarized in Table 1.

## 2. Numerical procedure

The mean flow is driven by the uniform pressure gradient with the passive scalar fields (see Figure 1). One of the thermal boundary conditions is the uniform heat-flux heating over the both surfaces (UHF), and the other is the constant temperature difference between the walls (CTD). Periodic boundary condition is imposed in the horizontal directions and non-slip condition is applied on the walls. For the air of Prandtl number  $Pr = 0.71$ , all fluid properties are treated

Table 1: Reynolds numbers and domain box-sizes of the present DNS: flow field with puff-like structure,  $\circlearrowright$ ; without puff,  $\times$ . Bulk mean velocity,  $u_m$ ; box-length in  $i$ -direction;  $L_i$ .

$Re_\tau (= u_\tau \delta / \nu)$	180	150	110	80	70	64	60 <sup>†</sup>	80	64	60
$Re_m (= u_m 2\delta / \nu)$	5680	4620	3270	2290	2000	1850	—	2310	1770	1640
with/without Puff	$\times$	$\times$	$\times$	$\times$	$\times$	$\times$	$\times$	$\circlearrowright$	$\circlearrowright$	$\circlearrowright$
Box size	Medium (MB)					Large (LB)		Extra-large (XL)		
$L_x \times L_y \times L_z$	$12.8\delta \times 2\delta \times 6.4\delta$					$25.6\delta \times 2\delta \times 12.8\delta$		$51.2\delta \times 2\delta \times 22.5\delta$		

<sup>†</sup> This case resulted in a laminarization.

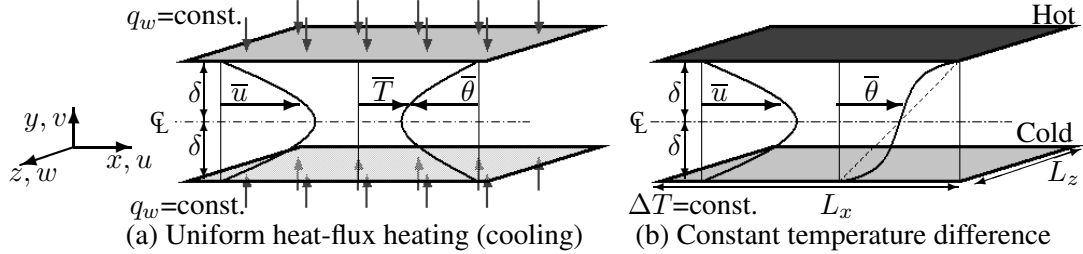


Figure 1: Configurations of the thermal boundary conditions.

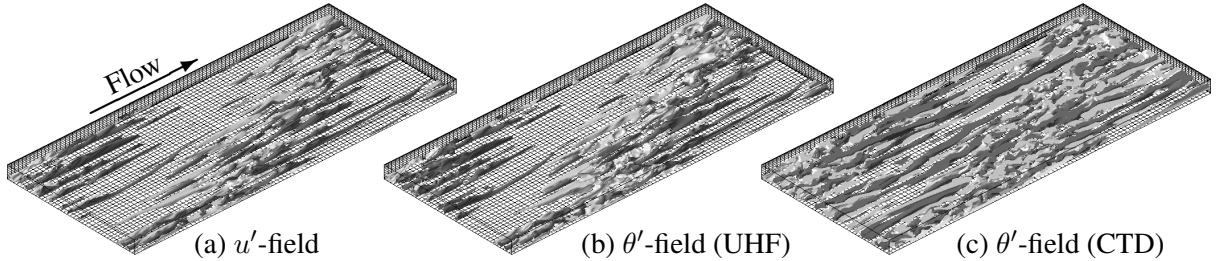


Figure 2: Instantaneous velocity and thermal fields for  $Re_\tau = 64$  (XL); high/low-speed (a) and high/low-temperature (b,c) regions (light-gray :  $u'^+, \theta'^+ \geq 3.0$ , dark-gray :  $u'^+, \theta'^+ \leq -3.0$ ). The visualized volume is the lower half of the computational box, namely  $51.2\delta \times \delta \times 22.5\delta$ .

as constant. The fundamental equations are the continuity, the Navier-Stokes and the energy equations. For the spatial discretization, the finite difference method is adopted. Further details of the method can be found in Kawamura *et al.* [2]. A fully developed flow field at a higher  $Re$  is successively used as the initial condition for a one-step lower  $Re$ . Note that various statistical data and visualized fields are obtained after the scalar fields reached statistical-steady state.

### 3. Results and Discussion

The puff-like structure as mentioned above is observed by the present DNS at much lower Reynolds numbers than  $Re_\tau = 80$ . Figure 2(a) shows the instantaneous flow field accompanied by the turbulent puff, which is equilibrium and stays constant in size for  $Re_\tau = 60 - 80$  (XL). The highly disordered turbulent region, in which streaks are densely crowded, is spatially distributed in the horizontal directions, although the turbulent puff of a pipe is intermittent only in streamwise direction [5]. We have confirmed that this oblique structure was able to be captured even if an initial velocity field was taken from a random condition. Thus one may regard the inclination of the puff-like structure as essential for the transitional channel flow. As can be seen from Table 1, to capture the puff in a channel requires a large-scale domain such as XL. Neither MB nor LB is large enough for the equilibrium to become established. It is interesting to note that the self-sustained puff in XL remains dominant with decreasing  $Re_\tau$  from 64 to

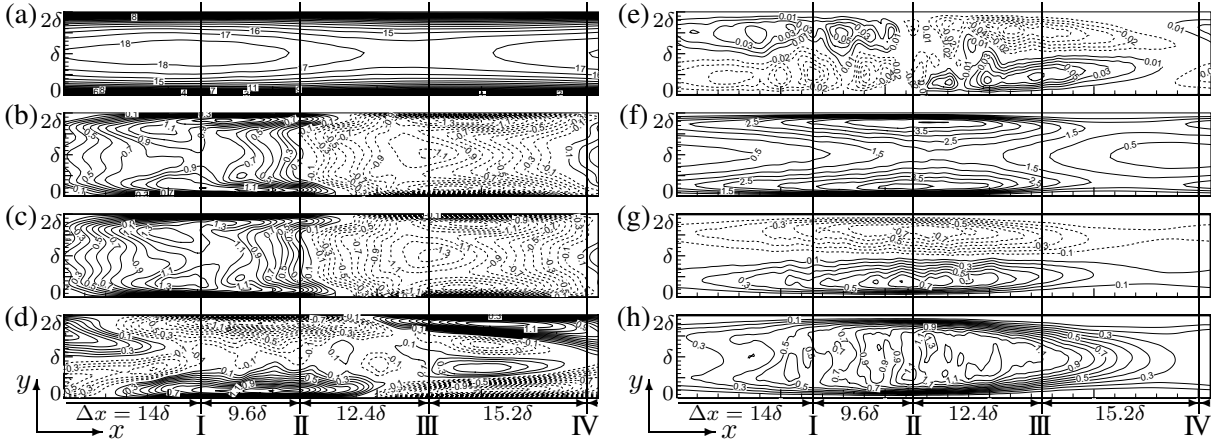


Figure 3: Quasi-mean flow and thermal fields of UHF (c, g) and CTD (d, h) in an ( $x$ - $y$ ) frame of reference moving with the puff; mean flow direction is from left to right. The ensemble-averaged pattern of (a) the quasi-mean streamwise velocity  $\bar{u}^{z'}$ , (b)  $\bar{u}^{z'} - \bar{u}$ , (c, d)  $\bar{\theta}^{z'} - \bar{\theta}$ , (e) the wall-normal component  $\bar{v}^{z'}$ , (f) the turbulent kinetic energy  $\bar{u''_i u''_i}/2^{z'}$  and (g,h) the wall-normal turbulent heat flux  $-\bar{v''\theta''}^{z'}$ , where all of quantities are normalized by  $u_\tau$  and/or a friction temperature. Solid and dashed lines represent positive and negative values, respectively.

60, while the turbulent flow has become laminar in the case of LB. From the visualization of the thermal fields affected by the puff, it is observed that thermal streaks in UHF are unevenly distributed and similar to the velocity field (Figure 2(b)). In the case of CTD, both high- and low-temperature regions exist uniformly in the core region, as shown in Figure 2(c).

Let us define  $z'$  as the coordinate which is parallel to the diagonal of the domain. A value spatial-averaged in the  $z'$ -direction and a fluctuation from the quasi-mean value are defined as:

$$\bar{u}_i^{z'}(x, y) = \iint u_i(x + t \cdot u_m, y, z', t) dz' dt, \quad u_i'' = u_i - \bar{u}_i^{z'}. \quad (1)$$

By assuming homogeneity of the puff in the  $z'$ -direction, the ensemble-averaged velocity and temperature fields with respect to the puff are obtained at  $Re_\tau = 64$  (XL) as given in Figure 3. Figures 3(a, b) show that the large-scale regions of the high- and low-speed fluctuations emerge occupying the whole width in the wall-normal direction. Moreover, at the interface between the upstream high-momentum (around the vertical-line I) and the downstream low-momentum regions (III), a strong-turbulent zone (II) appears as seen in Figure 3(f). On the other hand, for the area of III~IV~I, the reduction in the turbulent kinetic energy is caused by the local acceleration of the mean flow. The contour of UHF indicates a large-scale structure similar to that of the velocity field, while such structure cannot be found in the case of CTD (see Figure 3(c, d)). Figures 3(g, h) indicate that at the zone II, the wall-normal heat flux becomes as large as twice of its mean values in both of the thermal boundary conditions. This spatial intermittency of the heat transport is induced by the wall-normal secondary flow (Figure 3(e)).

The dimensionless mean velocity and temperature profiles are shown in Figure 4. An overline of  $\bar{u}$  denotes the spatial (in both  $x$  and  $z$  directions) and temporal averaging. For  $Re_\tau \leq 80$ , the Reynolds number dependence in the present DNS data is also consistent with the trend of the mean velocity profiles measured by Patel & Head [6]. If emphasis is placed on the data at  $Re_\tau = 80$  (MB and XL), their trends suggests that the maximum values of  $\bar{u}^+$  and  $\bar{\theta}^+$  increase with extending the box size up to XL, since the quasi-laminar region locally appeared in the flow

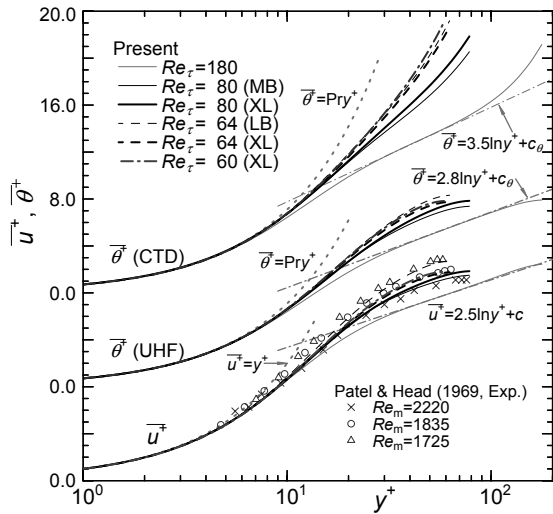


Figure 4: Mean velocity  $\bar{u}$  and temperature  $\bar{\theta}$  profiles in viscous wall-units.

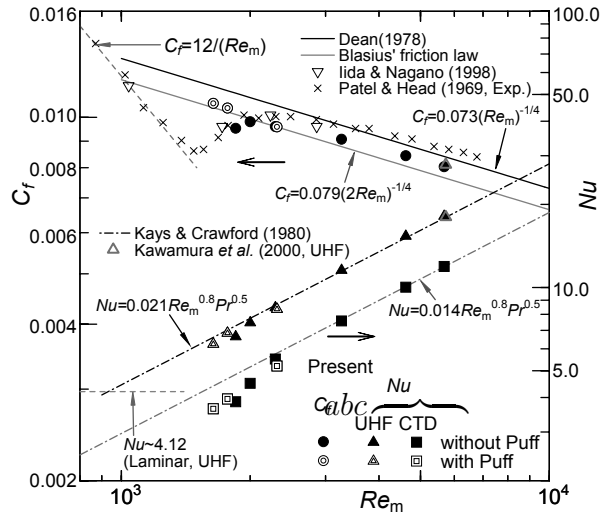


Figure 5: Variation with Reynolds number of  $C_f$  and  $Nu$ . Laminar flow relations, (---).

field. However, the Reynolds-number dependencies of both  $\bar{u}^+$  and  $\bar{\theta}^+$  in the flow subjected to the puff are significantly smaller than those without the puff. Figure 5 shows variations of the skin friction coefficient  $C_f$  and the Nusselt number  $Nu$  in comparison with the empirical correlations for a turbulent flow. As a result, both of  $C_f$  and  $Nu$  with the puff tend to be somewhat higher than those without puff, and stay closer to the empirical correlations even for very low Reynolds numbers.

## Acknowledgements

The present study is entrusted from Ministry of Education, Culture, Sports, Science and Technology of Japan, and the first author is supported by JSPS Research Fellowship for Young Scientists. The present computations were performed with the use of supercomputing resources at Information Synergy Center, Tohoku University.

## References

1. J. Kim and P. Moin, Transport of passive scalars in a turbulent channel flow. In *Turbulent Shear Flows 6* (Edited by J.-C. André et al.), Springer-Verlag, Berlin, pp. 85-96, 1989.
2. H. Kawamura, H. Abe and K. Shingai. DNS of turbulence and heat transport in a channel flow with different Reynolds and Prandtl numbers and boundary conditions. In *Third Int. Symp. on Turbulence, Heat and Mass Transfer* (Edited by Y. Nagano et al.), pp. 15-32, 2000.
3. O. Iida and Y. Nagano. The relaminarization mechanisms of turbulent channel flow at low Reynolds numbers. *Flow, Turbulence and Combustion*, 60: 193-213, 1998.
4. T. Tsukahara, Y. Seki, H. Kawamura and D. Tochio. DNS of turbulent channel flow at very low Reynolds numbers. In *Fourth Int. Symp. on Turbulence and Shear Flow Phenomena* (Edited by J.A.C. Humphrey et al.), pp. 935-940, 2005.
5. I. J. Wygnanski and F. H. Champagne. On transition in a pipe. Part 1. The origin of puffs and slugs and the flow in a turbulent slug. *J. Fluid Mech.*, 59: 281-335, 1973.
6. V. C. Patel and M. R. Head. Some observations on skin friction and velocity profiles in fully developed pipe and channel flows. *J. Fluid Mech.*, 38: 181-201, 1969.
7. R. D. Dean. Reynolds number dependence of skin friction and other bulk flow variables in two-dimensional rectangular duct flow. *J. Fluids Engng.*, 100: 215-222, 1978.
8. W.M. Kays and M.E.Crawford. In *Convective heat and mass transfer*, McGraw-Hill, 1980.